NASA Technical Memorandum 102879

Estimates of Thermochemical Relaxation Lengths Behind Normal Shock Waves Relevant to Manned Lunar and Mars Return Missions, the Aeroassist Flight Experiment, and Mars Entry

John T. Howe

February 1991

National Aeronautics and Space Administration

NASA Technical Memorandum 102879

Estimates of Thermochemical Relaxation Lengths Behind Normal Shock Waves Relevant to Manned Lunar and Mars Return Missions, the Aeroassist Flight Experiment, and Mars Entry

John T. Howe, Ames Research Center, Moffett Field, California

February 1991

National Aeronautics and
Space Administration

Ames Research Center
Moffett Field, California 94035-1000

SUMMARY

Thermochemical relaxation distances behind the strong normal shock waves associated with vehicles that enter the Earth's atmosphere upon returning from a manned lunar or Mars mission are estimated. The relaxation distances for a Mars entry are estimated as well, in order to highlight the extent of the relaxation phenomena early in currently envisioned space exploration studies. The thermochemical relaxation length for the Aeroassist Flight Experiment is also considered. These estimates provide an indication as to whether finite relaxation needs to be considered in subsequent detailed analyses. For the Mars entry, relaxation phenomena that are fully coupled to the flow field equations are used. The relaxation-distance estimates can be scaled to flight conditions other than those discussed.

NOMENCLATURE

A	Avogadro's number
c_{p_i}	specific heat at constant pressure for species i, per mole
$\bar{d}$	average diameter of two colliding particles
E_{f_r}	activation energy in forward-reaction-rate coefficient for reaction r
h	static enthalpy per unit mass
h_i	static enthalpy for species i, per mole
h_i^0	enthalpy of formation of species i, per mole
k	total number of species
k_{f_r}	forward-reaction-rate coefficient for reaction r
M	molecular weight
M	typical collision partner
M^*	reduced molecular weight ($1/M_i + 1/M_M$)
n_i	number of moles of species i per unit mass of mixture
P	sterric factor
p	static pressure

R	universal gas constant
s	number of classical squared terms of energy contributing to reaction
T	absolute temperature
u	velocity in x direction
X	a species
x	distance behind shock
α	reactant stoichiometric coefficient
β	product stoichiometric coefficient
ρ	mass density of mixture
ρ_0	standard or sea-level atmospheric density (1.225×10^{-3} g/cm^3)
σ	constant in equation (10)

Subscripts

eq	equilibrium value
f	forward
i	species i
M	typical collision partner
r	rth reaction
s	conditions immediately behind shock
0	reference condition at sea level (Earth)
∞	conditions ahead of shock

INTRODUCTION

Round-trip manned lunar and Mars missions may be the next major space exploration goals. For these missions, costly propulsive maneuvers will have to be replaced by more economical

aeromaneuvers in the upper atmosphere of Earth and the atmosphere of Mars. These aeromaneuvers will be performed as high as possible in the atmosphere to minimize heating of the vehicle while providing sufficient ambient atmospheric density to generate aeromaneuvering forces.

Hypervelocity flight in rarefied atmospheres raises questions concerning the thermochemical state of the flow field about flight vehicles. Although pioneering study over the past decade has been devoted to aeromaneuvering in the upper atmosphere of Earth (ref. 1) and to defining the thermochemical relaxation phenomena associated with flight speeds related to Earth orbital speeds (ref. 2), we must now begin to estimate the extent to which thermochemical relaxation phenomena pertain to prospective new missions. These missions (lunar and Mars return) are more energetic than Earth orbital missions and involve an atmospheric composition other than the Earth's (the Mars atmosphere). Also important is that the vehicles may be larger than those used to date. The estimates presented in the current report are especially timely because we are on the threshold of these new ventures.

To estimate the effects of phenomena that are largely beyond our experience, we extend previous experimental and analytical efforts, simplifying them to identify gross features. In the current report, thermochemical relaxation lengths behind normal shock waves will dominate the considerations.

AEROMANEUVERING IN EARTH ATMOSPHERE

Aeromaneuvering at hypervelocity in the upper atmosphere of Earth has been considered for more than two decades, and thermochemical relaxation phenomena in this regime have been studied intensely for the past decade. However, the foundation for these studies was laid about three decades ago with shock-tube experiments performed by Allen, Rose, and Camm (ref. 3). In those experiments, a high-speed shock wave was observed as it passed radiometric instrumentation at a station in the shock tube. In laboratory coordinates, the radiative intensity behind the moving shock wave increased to a peak value and then decayed to an "equilibrium" value at some distance behind the shock, for each test condition. Spectral measurements were also performed that were useful subsequently for devising molecular models of thermal nonequilibrium. The radiative pulse that peaked above an equilibrium value in the experiments was termed "nonequilibrium radiation." At the time the results were only of academic interest, primarily because the dominant heating of the Apollo capsule occurred at low altitudes where the atmospheric density was higher than the experimental density and the flow field about the vehicle was in equilibrium. However, the nonequilibrium radiative pulse behind the shock wave in the experiments contained the effects of both thermodynamic and chemical nonequilibrium phenomena and represented the coupled thermochemical relaxation behind the shock wave—the subject of intense study in recent years. For the current estimates of thermochemical relaxation effects, the data can be used directly.

Reference 3, figure 10, plots the product of pressure and the laboratory time after the shock wave passes to reach within 10% of thermochemical equilibrium (the ordinate) as a function of shock-wave velocity (the abscissa) for a large range of flight conditions in the Earth's atmosphere. The plot can be transformed into the corresponding relaxation length behind a normal shock wave. The result appears in figure 1 as three lines near the top center of the figure, labeled 1 cm, 10 cm, and 100 cm.

These lines are the loci of the thermochemical relaxation lengths. Some flight trajectories, and other information, appear on the figure, to relate the relaxation regime to flight experience. Of particular interest is the Aeroassist Flight Experiment (AFE) trajectory. The AFE will examine thermochemical relaxation phenomena and their effects, for developing Aeroassist Space Transportation Vehicles (ASTV). Such vehicles, which will move space payloads from one orbit to another in Earth–Moon space, requiring changes in both orbital altitude and orbital plane inclination, will function in the AFE domain. The figure shows that for the AFE at peak heating, the thermochemical relaxation length behind a normal shock wave is about 10 cm. That is a significant part of the shock layer because the bow shock is about 17 cm in front of the vehicle. Thus a large fraction of the AFE forebody flow field is out of equilibrium thermochemically, which is the intent of the experiment.

In figure 1, the point of peak heating on a lunar return vehicle lies below the perigee of the AFE. The lunar return vehicle would enter and maneuver in the Earth's upper atmosphere, similarly to the ASTV, and exit the atmosphere to rendezvous with a vehicle in Earth orbit. The figure shows that for this vehicle, the thermochemical relaxation length behind a normal shock wave is estimated to be between 1 and 10 cm—say about 5 cm. For a large, drag-configured vehicle, the thermochemical relaxation length would be of some significance if the shock layer were much thicker than 5 cm, but its effects would not dominate the forebody flow field. Thus the importance of the thermochemical relaxation phenomena can be estimated from the geometry and size of the prospective lunar return vehicle.

Finally, consider the entry into the Earth's atmosphere of a manned Mars return vehicle. It may perform an aerocapture maneuver as shown in figure 1, or it may descend to Earth. The entry velocity is large, about 14 km/sec. (That speed also includes an emergency abort entry.) The vehicle is very energetic, and it experiences peak heating lower in the atmosphere than the other vehicles discussed. It is estimated that the thermochemical relaxation distance behind a normal shock wave is less than 1 cm, and its effects may be relatively unimportant, depending on the thickness of the forward shock layer.

AEROMANEUVERING IN THE MARS ATMOSPHERE

The composition of the Mars atmosphere is considered to be about 95% CO_2 and 5% N_2 (ref. 4). The density of the flight domain is low and thermochemical relaxation should be examined. Because the dominant atmospheric species is considered to be CO_2, it is useful to note some features of the basic global conservation equations for compressible flow of CO_2 along a streamline where transport phenomena are neglected, but relaxation phenomena are allowed. The conservation equations for mass, momentum, and energy for the steady state are, respectively,

$$\rho\frac{du}{dx}+u\frac{d\rho}{dx}=0 \tag{1}$$

$$\rho u\frac{du}{dx}=-\frac{d\rho}{dx} \tag{2}$$

$$u\frac{du}{dx}+\frac{dh}{dx}=0 \tag{3}$$

In the absence of relaxation processes, a solution of these equations is that all variables—velocity (u), density (ρ), pressure (p), and static enthalpy (h)—are constant. However, for a relaxing flow field behind a strong normal shock wave in which the density behind the shock is much larger than that ahead of the shock, it can be shown from these equations which variables are most sensitive to any process that occurs in the flow; density and velocity can be affected significantly, but pressure and static enthalpy are affected very little. This can be shown without solving the equations or specifying the process. The process enters the problem through the equation of state and whatever supplemental equations describe the process. Also, since pressure is relatively invariant and density is potentially highly variable, temperature is highly variable because of the equation of state. Although this argument is simple, it is not obvious or intuitive, and examples that illustrate the sensitivity will be provided in the following sections. The concept is useful because before solving the equations, the relative behavior of the global flow and thermodynamic variables can be anticipated. This knowledge may affect the formulation of the method of solving the equations, the devising of numerical algorithms, and perhaps the determination of whether a solution can be obtained at all. Thus, for the current approach, we know that it is not necessary to deal with large excursions in pressure or static enthalpy caused by relaxation processes.

Thermal Relaxation

In an early analysis by Howe and Sheaffer of thermochemically relaxing flow in a predominantly CO_2 atmosphere, each species was allowed to assume various levels of thermal excitation parametrically, with no mechanism for thermal relaxation (ref. 5). The analysis showed that the effects of thermal excitation on both the flow field and the distribution of chemical species was insignificant. (At the time, the study in ref. 5 was not specifically related to Mars entry because the Mars atmosphere was estimated to contain less than 10% CO_2, as noted in refs. 6 and 7).

A subsequent analysis by Hindelang of thermochemical relaxation behind strong shock waves in CO_2 showed that the effects of vibrational relaxation and vibration–dissociation coupling are much stronger in CO_2, which has three different vibrational modes, than in diatomic gases, which have only a single mode (ref. 8). However, at shock speeds greater than 6 km/sec, the process of finite-rate dissociation of CO becomes dominant, and the region of CO_2 relaxation is only a small part of the overall relaxation region. Thermally, vibrational relaxation does not have a significant effect on the flow field at these higher speeds.

Recently, Candler obtained a detailed two-dimensional solution for the forebody flow fields of vehicles flying at speeds of 6.1 to 7.4 km/sec in the Mars atmosphere, in ambient densities of the order of 10^{-4} kg/m^3 (ref. 9). Thermally, two temperatures (translational and vibrational) were considered; chemically, 12 reactions and their "reverse" reactions were considered. Thermochemically, the flow field was allowed to relax at a finite rate. Candler concluded that "for the cases studied, there is very little thermal nonequilibrium due to the very fast vibrational relaxation of CO_2." Although this analysis considered the elements C, O, and N, it confirmed the results of the early analyses which were limited to C and O (refs. 5 and 8).

For estimating relaxation lengths, the balance of this study will be limited to chemical relaxation in a predominantly CO_2 atmosphere.

Chemical Relaxation

To proceed with estimates of the chemical relaxation lengths behind strong normal shock waves in CO_2, we write the equation of state for the mixture of CO_2 and its components as

$$p = \rho RT \sum_{i=1}^{k} n_i \tag{4}$$

where the summation is over all involved species. It is assumed, because of the analyses described in the preceding section, that chemical relaxation is characterized by the translational temperature. The static enthalpy of each species is

$$h_i = h_i^0 + \int_0^T c_{p_i}\, dT \tag{5}$$

and the static enthalpy of the relaxing mixture is

$$h(p,\rho,n_i,\ldots,n_k) = \sum_{i=1}^{k} n_i h_i \tag{6}$$

For each reaction r that involves species i, the chemical reactions that pertain to the relaxing flow field can be expressed as

$$\sum_{i=1}^{k} \alpha_{r,i} X_i \xrightarrow{k_{f_r}} \sum_{i=1}^{k} \beta_{r,i} X_i \tag{7}$$

where the arrow indicates that the reaction proceeds to the right at a rate characterized by k_{f_r}. (It is possible, but not generally true, that the reverse reaction is also allowed; for example, the oxidation of carbon monoxide in a single step is unlikely in this context.)

For each species, the variation along the streamline can be written by manipulating equations (1)–(7) to form

$$\frac{dn_i}{dx} = \frac{1}{\rho u} \sum_{r} (\beta_{r,i} - \alpha_{r,i}) k_{f_r} \left[\prod_{i} (\rho n_i)^{\alpha_{r,i}} \right] \tag{8}$$

Equation (8) shows that the relaxation process is coupled to the flow field, and the analysis should include flow-field variations that interact with the relaxation process.

For current purposes, we can allow c_{p_i}/R to be constant for each species. The following expression can then be derived from equations (1)–(3) and (5)–(6) (see ref. 10):

$$\frac{du}{dx} = \left[\frac{u}{1 - \rho u^2 \sum_{i=1}^{k} n_i \left(\frac{c_{p_i}}{R} - 1 \right) \Big/ p \sum_{i=1}^{k} n_i \frac{c_{p_i}}{R}} \right] \times \left[\left(\sum_{i=1}^{k} \frac{dn_i}{dx} \Big/ \sum_{i=1}^{k} n_i \right) - \left(\sum_{i=1}^{k} \frac{c_{p_i}}{R} \frac{dn_i}{dx} \Big/ \sum_{i=1}^{k} n_i \frac{c_{p_i}}{R} \right) - \left(\sum_{i=1}^{k} h_i^0 \frac{dn_i}{dx} \Big/ RT \sum_{i=1}^{k} n_i \frac{c_{p_i}}{R} \right) \right] \tag{9}$$

(This differential equation was modified in reference 8 to account for vibrational relaxation.) Equation (9) is solved for chemical relaxation behind a strong normal shock wave by use of equation (8), which is solved for each species that is participating in the rth reaction at a rate given by

$$k_{f_r} = 2\left[PA\bar{d}^2/\sigma(s-1)! \right] (2\pi RT/M^*)^{1/2} (E_{f_r}/RT)^{s-1} e^{-(E_{f_r}/RT)} \tag{10}$$

This form of the reaction coefficient highlights several physical quantities that need to be determined (or estimated): P, the sterric factor; s, which is related to the number of contributing energy modes; and E_{f_r}, the activation energy for the reaction. For a gas that is relaxing thermally and is characterized by more than one temperature, this expression is difficult to evaluate meaningfully. For a single temperature, the behavior of the expression can be examined parametrically, and judgments can be made that have some physical meaning. This was done for CO_2 and its components at a time when no experimental results were available to the author (refs. 5 and 10), and the results are compared in figure 2 with experimental results. For current purposes, only density ratios of the order of $\rho_\infty/\rho_0 \approx 10^{-4}$ are of interest. The flight speeds of interest are from 6 to 9 km/sec; these two speeds are shown at the top of the figure with their corresponding temperature ranges, to orient the reader. Two reactions are shown in the figure:

$$CO_2 + M \rightarrow CO + O + M \tag{11}$$

$$CO + M \rightarrow C + O + M \tag{12}$$

where M is any typical collision partner. The second reaction, equation (12), may be a global reaction. Its steps were reported by Fairbairn to include the formation and dissociation of C_2 (ref. 11), although for the elevated temperatures under consideration, that is a rather surprising concept. However, the rate coefficients used in the current report are shown by the solid lines in the figure. The

rate coefficient for reaction (11) is compared in the figure with the experimental data of Brabbs, Belles, and Zlatarich (ref. 12) at a temperature below the range of interest. The predicted rate coefficients for both reactions are also compared with the shock-tube data of Davies (refs. 13 and 14). At the temperatures of interest, the estimate of the CO dissociation rate is close to the measurements of Davies. The estimate of the CO_2 dissociation rate is higher than Davies' result at about 11,000 K and is close to but lower than Davies' result at about 6000 K. In the following analysis, the estimates of the forward-reaction rates will be used to estimate relaxation lengths. Generally, the relaxation lengths will be close to but less than those that would be predicted by use of Davies' data.

A solution for the chemically reacting flow field in CO_2 is shown in figure 3 for a flight speed of 6 km/sec at ambient density ratio $\rho_\infty/\rho_0 = 10^{-4}$ (adapted from ref. 10). The distance behind the shock is measured along the abscissa, with $x = 0$ representing the shock location. The distance scale is broken in order to capture the variations just behind the shock wave as well as those far downstream of the shock. (A log scale was not used because of the singularity at $x = 0$.) On the right side of figure 3(a), the ratios of equilibrium values to values just behind the shock are shown for the variables ρ, p, u, and T. Density, velocity, and temperature vary significantly in the flow field, as predicted previously in the current paper, and pressure and static enthalpy do not. Figure 3(b) shows that for this flight condition, only the dissociation of CO_2 to CO and O is important. The dashed curves represent an analytic solution wherein the chemistry is uncoupled from the flow field, as described in reference 10.

Figure 4 displays the solution for a higher flight speed: 9 km/sec. The dissociation of both CO_2 and CO are important at this speed, which is more than twice as energetic as the previous example, and the analytic approximation does not represent the chemical variation as well as at 6 km/sec.

At 9 km/sec, the flow field is sufficiently energetic to partially ionize the reacting mixture; a solution that includes ionization is shown in figure 5 (which was adapted from ref. 5). In that solution, five reactions were included, some of which were ionizing reactions. The ionizing-reaction-rate coefficients were also estimated, but are not assessed for their validity in the current paper. The variations caused by ionization can be seen by comparing figure 5 with figure 4. It may be noted in figure 5 that ionized species sometimes overshoot their equilibrium values in the hot part of the relaxing flow field, as do other species. These overshoots can affect the gaseous radiation and other phenomena.

Figure 6 shows the combined results of many solutions to the problem of chemical relaxation, in terms of relaxation length. In this figure the percentage of the total molar change required to achieve chemical equilibrium is plotted as a function of distance (or length) behind the normal shock wave. Three curves are shown, one for each of three flight velocities, at ambient density $\rho_\infty/\rho_0 = 10^{-4}$. The curve for 6 km/sec contains primarily the effects of CO_2 dissociation (see fig. 3(b)). We may infer from figure 5 that the curve for 8 km/sec reflects the dissociation of both CO_2 and CO, and a very small degree of ionization (ionization-solution results from ref. 5 were included). The 10 km/sec curve also reflects the dissociation of both CO_2 and CO, and the degree of ionization for this curve was significant. However, the effect of ionization on chemical relaxation length was insignificant, possibly because the reactions proceeded more rapidly at this more energetic flight speed (within the limitations of this approximate formulation). Note that the curve for 6 km/sec crosses that for 8 km/sec. For progressively lower flight speeds, the crossing may be expected to progress leftward,

and in the limiting case of compressible flow that is not reacting chemically, the curves would cross at a relaxation length of zero. We must not speculate too freely, however, because the problem is coupled and nonlinear, and the inputs are uncertain estimates. Suffice it to say that the curves cross. Also note that for the flight conditions and for all flight speeds shown in figure 6, 90% of the chemical relaxation is complete on the order of 10 cm behind the shock wave.

A careful examination of results in references 5 and 10 leads to the plot in figure 7, which shows the chemical relaxation length as a function of flight speed at $\rho_\infty/\rho_0 = 10^{-4}$. Here, relaxation length corresponds to the location where 90% of the chemical relaxation is achieved. The relaxation length peaks at about 54 cm at a flight speed of about 7.5 km/sec. M. E. Tauber calculated peak heating at 7.7 km/sec at density ratio $\rho_\infty/\rho_0 = 1.24 \times 10^{-4}$ (private communication, Ames Research Center, 1990). To the extent that binary scaling applies, the chemical relaxation length scaled from figure 7 would be 54 cm/1.24 = 43 cm.

The estimates of the chemical relaxation length behind a normal shock wave in CO_2 at an ambient density of the order of $\rho_\infty/\rho_0 = 10^{-4}$ at flight speeds of about 7 km/sec are dominated by the dissociation of CO_2 and CO. The estimates are probably meaningful because dissociation rates are available. The rate used in the analysis for CO dissociation is close to the measured rate, while that for CO_2 dissociation is near or higher than the measured rate. Although the latter may make the estimates conservative, the CO_2 dissociates so rapidly that the estimate of the overall length is probably affected very little. In any event, these estimates can be refined when more accurate information is acquired or when other refinements or judgments are made.

Finally, shock-tube measurements related to nonequilibrium flow behind normal shock waves in CO_2 for a hypothetical high-speed entry into the Venus atmosphere were made by Nealy (ref. 15). The nonequilibrium radiative-intensity waveform behind the shock wave was recorded at a wavelength of 158 nm. The time for the intensity to peak and then decay to half the difference between peak and equilibrium levels was measured. C. Park scaled a corresponding partial relaxation length from this data; for a shock velocity of 10 km/sec at $\rho_\infty/\rho_0 = 5 \times 10^{-4}$, it was about 12.5 cm (private communication, Ames Research Center, 1990). Binary scaling for $\rho_\infty/\rho_0 = 10^{-4}$ yields a partial relaxation length of 5×12.5 cm = 62.5 cm. Although a rigorous comparison with figures 6 and 7 is not feasible, the relaxation length inferred from the experiments is large—probably larger than the present estimate at that high-speed condition, and perhaps two or three times that value. The conclusion that nonequilibrium flow is significant and should be considered in Mars flow-field analyses is thus reinforced by both analysis and experiment.

CONCLUDING REMARKS

Estimates of thermochemical relaxation lengths behind normal shock waves in air and CO_2 were made, to assess the significance of nonequilibrium phenomena in studies of forebody flow fields for hypervelocity aeromaneuvering in the atmospheres of Earth and Mars. For Earth the thermochemical relaxation length is a large fraction of the bow-shock standoff distance for the Aeroassist Flight Experiment currently being planned. That is desirable because one of the objectives of the experiment is to study the nonequilibrium phenomena. For manned return from the Moon to Earth by use

of aeromaneuvering vehicles, thermochemical relaxation may be insignificant near peak heating if the vehicle configuration is large and blunt. For the manned Mars return aerocapture maneuver, thermochemical relaxation near peak heating seems to be of little importance.

Thermodynamic relaxation for entry into the Mars atmosphere seems to be of little importance on the vehicle forebody for flight conditions of current interest. On the other hand, the chemical relaxation length seems to be significant. It is estimated to be about half a meter at peak heating. This result can be scaled to other flight conditions.

REFERENCES

1. Menees, G. P.: Design and Performance Analysis of an Aeromaneuvering Orbital-Transfer Vehicle Concept. IAF Paper 85-139, 1985.

2. Park, C.: Calculation of Nonequilibrium Radiation in AOTV Flight Regimes. AIAA Paper 84-0306, 1984.

3. Allen, R. A.; Rose, P. H.; and Camm, J. C.: Nonequilibrium and Equilibrium Radiation at Super-Satellite Re-entry Velocities. AVCO Everett Research Laboratory Research Report 156, Sept. 1962.

4. Seiff, A.; and Kirk, D. B.: Structure of the Atmosphere of Mars in Summer at Mid-Latitudes. J. Geophys. Res., vol. 82, no. 28, Sept. 1977, pp. 4364-4378.

5. Howe, J. T.; and Sheaffer, Y. S.: Chemical Relaxation Behind Strong Normal Shock Waves in Carbon Dioxide Including Interdependent Dissociation and Ionization Processes. NASA TN D-2131, 1964.

6. Howe, J. T.; and Viegas, J. R.: Dissociative Relaxation of CO_2 Behind Normal Shock Waves. Paper presented at Interplanetary Missions Conference of 9th Annual American Astronautical Society Meeting at Los Angeles, Jan. 1963.

7. Kaplan, L. D.: A Preliminary Model of the Venus Atmosphere. Tech. Rep. 32-379, Jet Propulsion Lab., Pasadena, CA, Dec. 1962.

8. Hindelang, F. J.: Coupled Vibration and Dissociation Relaxation Behind Strong Shockwaves in Carbon Dioxide, NASA TR R-253, 1967.

9. Candler, G.: Computation of Thermo-Chemical Nonequilibrium Martian Atmospheric Entry Flows. AIAA Paper 90-1695, 1990.

10. Howe, J. T.; Viegas, J. R.; and Sheaffer, Y. S.: Study of the Nonequilibrium Flow Field Behind Normal Shock Waves in Carbon Dioxide. NASA TN D-1885, 1963.

11. Fairbairn, A. R.: The Dissociation of Carbon Monoxide. Proc. Roy. Soc. (London) A 312, 207, 1969.

12. Brabbs, T. A.; Belles, F.; and Zlatarich S.: Shock Tube Study of Carbon Dioxide Dissociation Rate. J. Chem. Phys., vol. 38, no. 8, Apr. 1963, pp. 1939-1944.

13. Davies, W. O.: Radiative Transfer on Entry into Mars and Venus. (NASA Grant N64-29185) NASA CR-58574, 1964.

14. Davies, W. O.: Carbon Dioxide Dissociation at 6000 to 110000 K. J. Chem. Phys., vol. 43, 1965, p. 2809.

15. Nealy, J. E.: An Experimental Study of Ultraviolet Radiation Behind Incident Normal Shock Waves in CO_2 at Venusian Entry Speeds. AIAA Paper 75-1150, 1975.

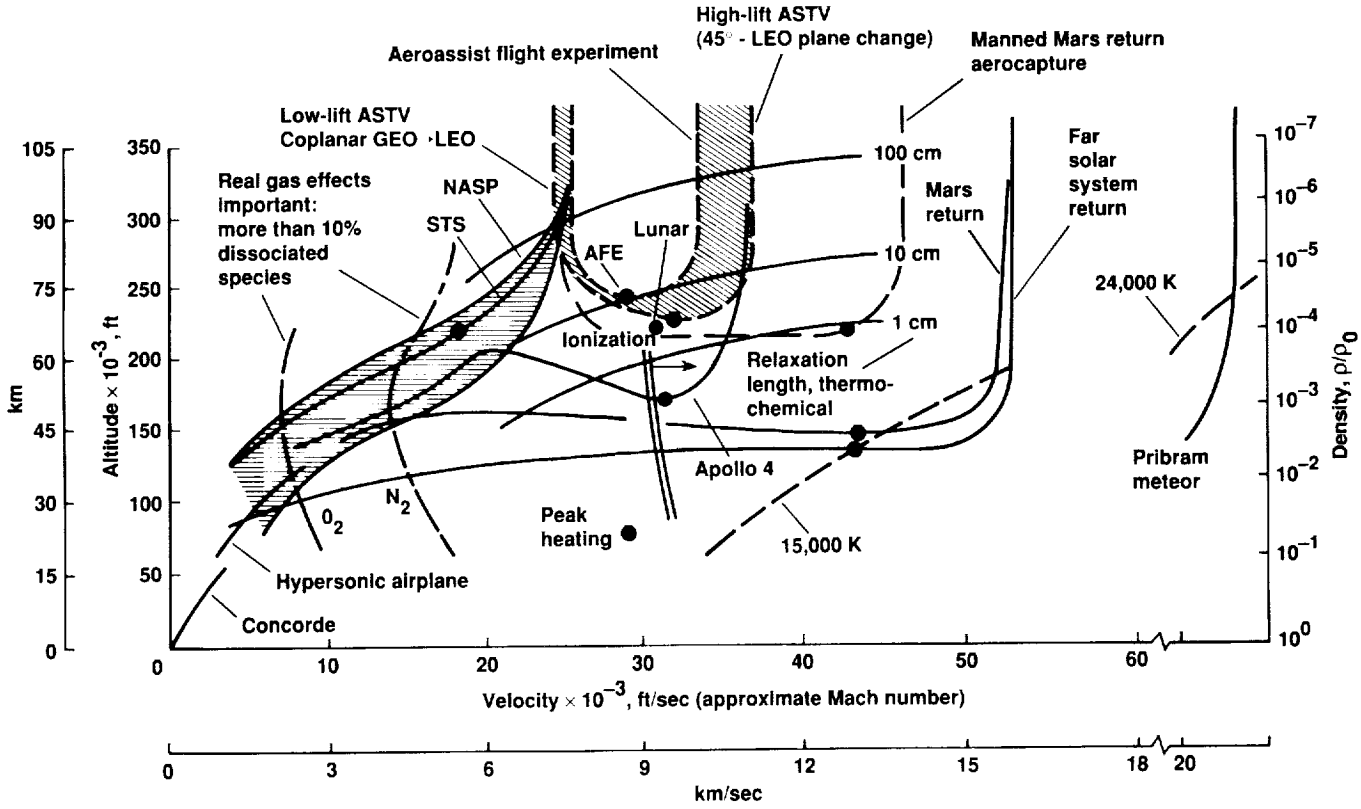

Figure. 1 The Earth aerothermodynamic flight regime, with the thermochemical relaxation domain highlighted.

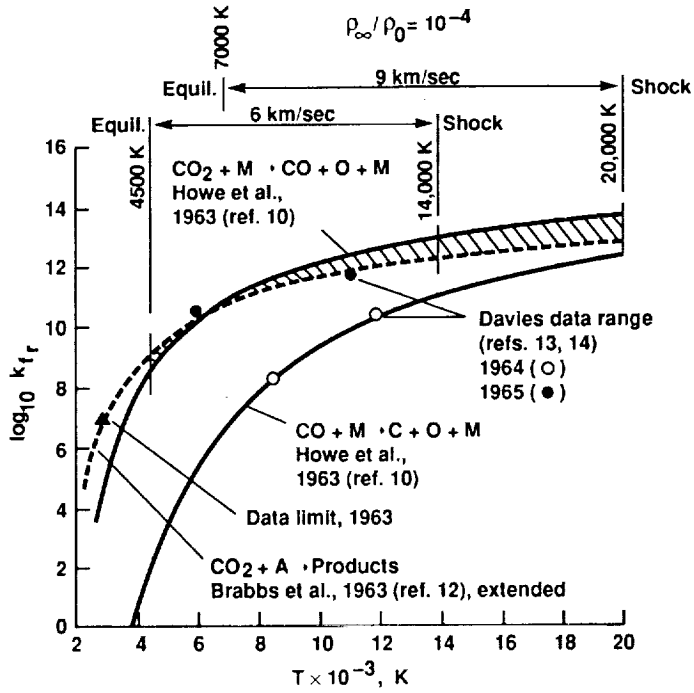

Figure 2. Forward-reaction-rate coefficients.

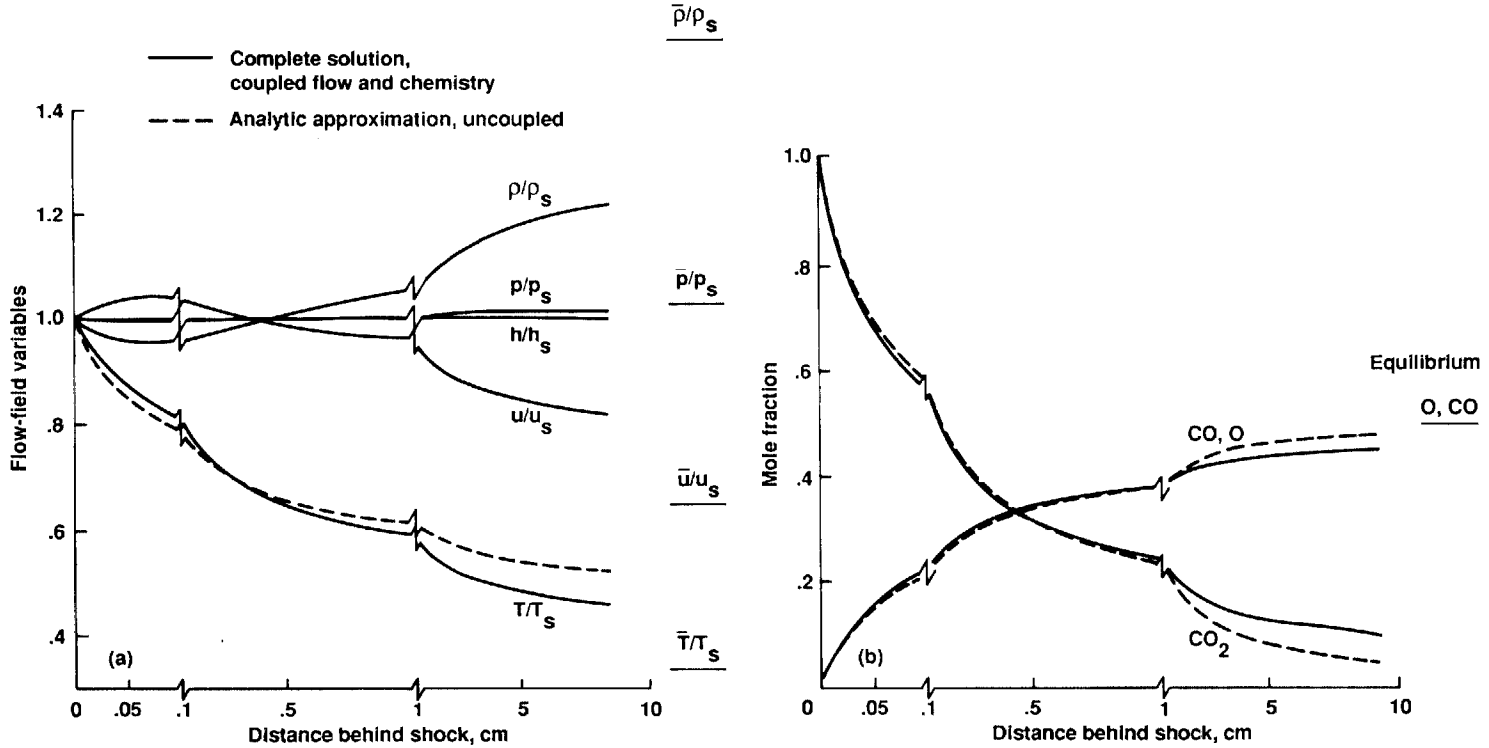

Figure 3. Nonequilibrium flow-field profiles; $u_\infty = 6$ km/sec, $\rho_\infty/\rho_0 = 10^{-4}$.

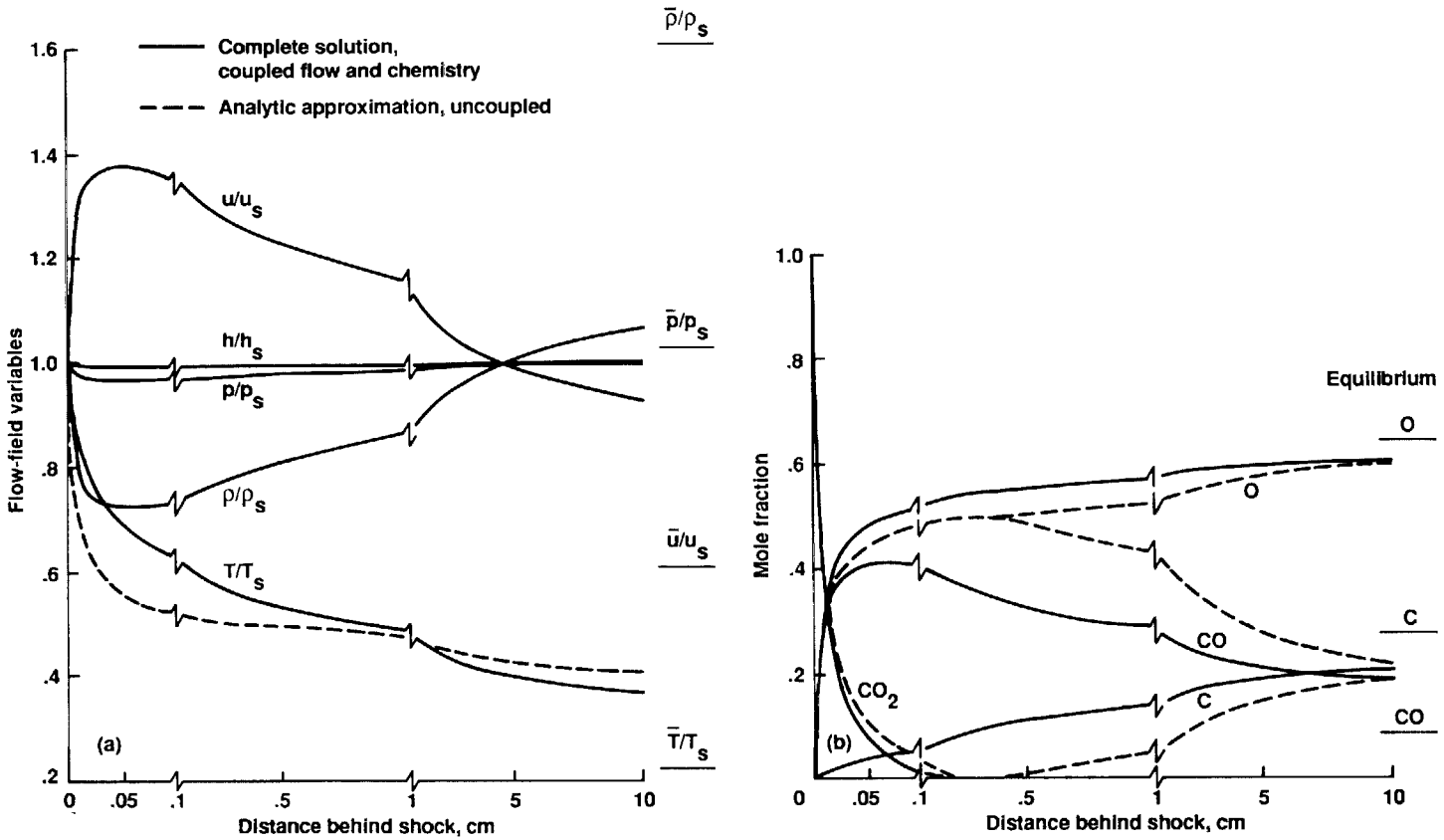

Figure 4. Nonequilibrium flow-field profiles; $u_\infty = 9$ km/sec, $\rho_\infty/\rho_0 = 10^{-4}$.

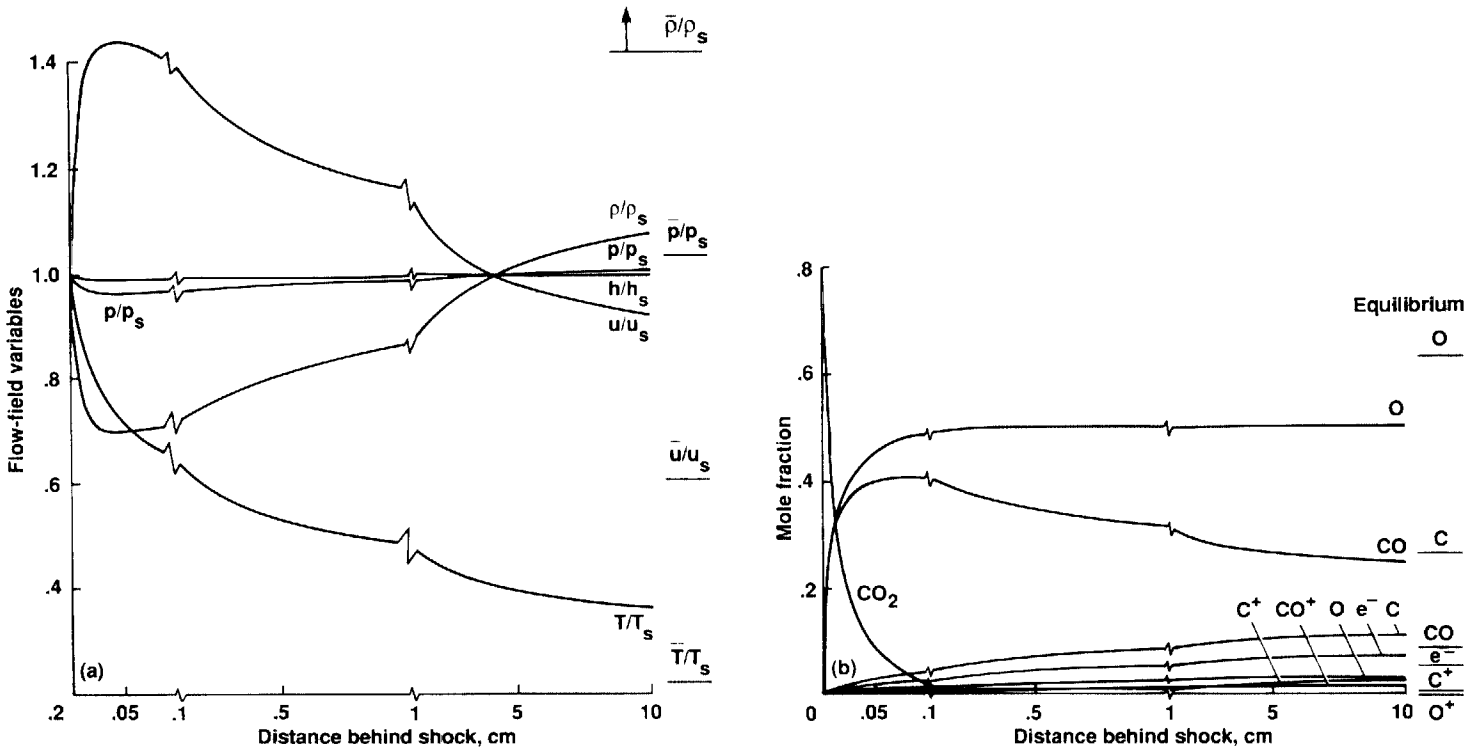

Figure 5. Nonequilibrium flow-field profiles with ionization; $u_\infty = 9$ km/sec, $\rho_\infty/\rho_0 = 10^{-4}$.

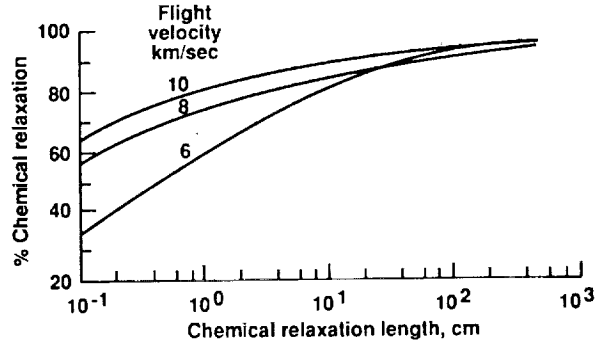

Figure 6. Relaxation length behind normal shock wave in CO_2—flow field coupled to chemistry; $\rho_\infty/\rho_0 = 10^{-4}$.

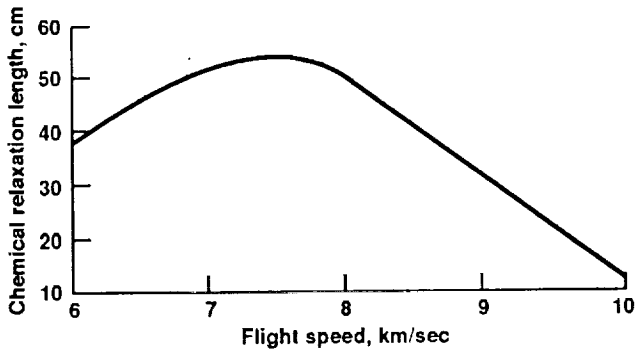

Figure 7. Chemical relaxation length (for 90% relaxation) behind normal shock wave in CO_2; $\rho_\infty/\rho_0 = 10^{-4}$.

NASA
National Aeronautics and Space Administration

Report Documentation Page

1. Report No.	2. Government Accession No.	3. Recipient's Catalog No.
NASA TM-102879		

4. Title and Subtitle

Estimates of Thermochemical Relaxation Lengths Behind Normal Shock Waves Relevant to Manned Lunar and Mars Return Missions, the Aeroassist Flight Experiment, and Mars Entry

5. Report Date

February 1991

6. Performing Organization Code

7. Author(s)

John T. Howe

8. Performing Organization Report No.

A-91003

10. Work Unit No.

506-40-91

9. Performing Organization Name and Address

Ames Research Center
Moffett Field, CA 94035-1000

11. Contract or Grant No.

13. Type of Report and Period Covered

Technical Memorandum

12. Sponsoring Agency Name and Address

National Aeronautics and Space Administration
Washington, DC 20546-0001

14. Sponsoring Agency Code

15. Supplementary Notes

Point of Contact: John T. Howe, Ames Research Center, MS 229-3, Moffett Field, CA 94035-1000
(415) 604-6113 or FTS 464-6113

16. Abstract

Thermochemical relaxation distances behind the strong normal shock waves associated with vehicles that enter the Earth's atmosphere upon returning from a manned lunar or Mars mission are estimated. The relaxation distances for a Mars entry are estimated as well, in order to highlight the extent of the relaxation phenomena early in currently envisioned space exploration studies. The thermochemical relaxation length for the Aeroassist Flight Experiment is also considered. These estimates provide an indication as to whether finite relaxation needs to be considered in subsequent detailed analyses. For the Mars entry, relaxation phenomena that are fully coupled to the flow field equations are used. The relaxation-distance estimates can be scaled to flight conditions other than those discussed.

17. Key Words (Suggested by Author(s))	18. Distribution Statement
Aerothermodynamics Thermochemically relaxing flow fields	Unclassified-Unlimited Subject Category - 34

19. Security Classif. (of this report)	20. Security Classif. (of this page)	21. No. of Pages	22. Price
Unclassified	Unclassified	20	A02